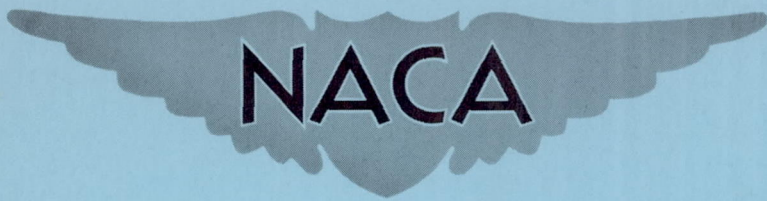# NACA

RESEARCH MEMORANDUM

THE PATH AND MOTION OF SCALE MODELS OF JETTISONABLE NOSE

SECTIONS AT SUPERSONIC SPEEDS AS DETERMINED FROM

AN INVESTIGATION IN THE LANGLEY

FREE-FLIGHT APPARATUS

By Lawrence J. Gale

Langley Aeronautical Laboratory
Langley Air Force Base, Va.

NATIONAL ADVISORY COMMITTEE
FOR AERONAUTICS

WASHINGTON
May 23, 1950
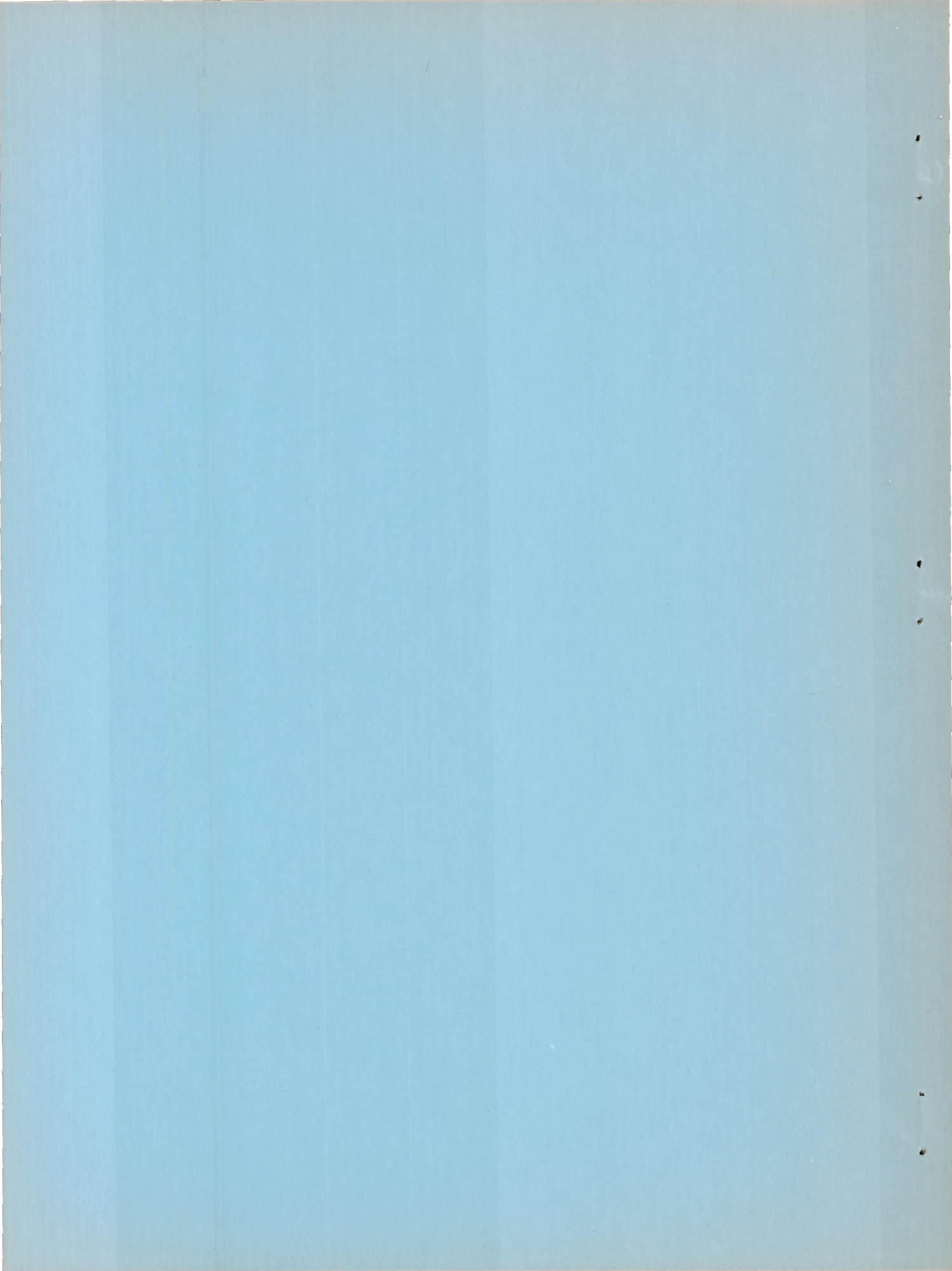
NATIONAL ADVISORY COMMITTEE FOR AERONAUTICS

———

RESEARCH MEMORANDUM

———

THE PATH AND MOTION OF SCALE MODELS OF JETTISONABLE NOSE

SECTIONS AT SUPERSONIC SPEEDS AS DETERMINED FROM

AN INVESTIGATION IN THE LANGLEY

FREE-FLIGHT APPARATUS

By Lawrence J. Gale

SUMMARY

An investigation has been conducted on models of two different designs of jettisonable nose sections wherein the nose sections have been projected at supersonic speeds (Mach number ranged from 1.2 to 1.4) in the Langley free-flight apparatus. Both nose designs in the original unstabilized (without-fins) condition turned away from a nose-first flight attitude and calculations indicated that a pilot within corresponding full-scale nose sections would encounter large accelerations (12 negative g for 0.014 second for one nose design and 26 negative g for 0.013 second for the other) as a result of this instability. Both nose designs with fins installed appeared stable, and calculations indicated that the equivalent motion in a corresponding full-scale nose section would not subject the pilot to large accelerations (6 transverse g).

INTRODUCTION

One of the problems confronting airplane designers of high-speed aircraft is safe pilot escape in an emergency. The conventional method of escape utilized from low-speed aircraft appears impractical in airplanes flying at supersonic speeds. A method of pilot escape from high-speed aircraft now being considered is that of jettisoning the nose section of the airplane in which the pilot is seated.

On the basis of results of low-speed investigations (references 1, 2, 3, and unpublished data), it has been determined that jettisonable nose sections not stabilized with fins will turn away from a nose-first flight attitude when released from an airplane. The size fins required to

stabilize various nose sections at low speeds has been determined (reference 1). In order to verify the unstable tendencies of nose sections, to check the stabilizing properties of fins when nose sections are jettisoned at supersonic speeds, and to determine whether the motions of the nose jettisoned at such speeds will cause large accelerations on the pilot, an investigation has been conducted in the Langley free-flight apparatus on two typical jettisonable nose sections, each with and without stabilizing fins. The nose sections were projected at Mach numbers ranging from 1.20 to 1.40.

Although the present investigation is concerned only with stabilization of a nose section at supersonic speeds, other test results (references 2 and 3) have shown that the separation of the nose from the remainder of the airplane can also present a serious problem and must be given serious consideration.

SYMBOLS

t time, seconds

c_0, c_1, c_2 coefficients for cubic equation

s distance, feet

W weight, pounds

a acceleration at center of gravity, feet per second^2

g gravitational acceleration, feet per second^2

m mass, slugs

ρ air density, slugs per cubic foot

A cross-sectional area of model at break-off station
                        (figs. 1 to 4), square feet

V flight velocity, feet per second

F force, pounds

I_X, I_Y, I_Z moments of inertia about X, Y, and Z body axes,
                        respectively, slug-feet^2

l linear dimension, feet

R   scale ratio, ratio of any dimension of full-scale nose
                   section to corresponding dimension of model nose section

r   distance from the center of gravity of a nose section to
                   pilot's head (figs. 1 and 2)

M   Mach number

ω angular velocity, radians per second

q   angular velocity in pitch, radians per second

K   ratio of velocity of sound at given altitude to velocity
                   of sound at sea level $\left(\left(\dfrac{V_{alt}}{V_o}\right)_{M=1}\right)$

C_D drag coefficient

Subscripts:

fs   full-scale

m   model

alt   altitude

o   sea level

METHODS AND APPARATUS

Apparatus, Testing Technique, and Reduction of Data

The Langley free-flight apparatus is a tank 100 feet in length
and 8 feet in diameter containing air or other test gases through
which models are projected at high speeds by means of a catapulting
mechanism. Precise records of the model time-space coordinates are
made. Space values are determined by the use of cameras mounted
at 10-foot intervals along the length of the tank and by the use
of shadowgraph apparatus located between some of the cameras. Time
values are determined by the use of a thermostatic crystal-controlled
oscillator which controls timing marks on a cathoderay oscillograph.
This oscillograph is photographed by a high-speed camera. At each
camera station, two exposures on each film are made as the model

crosses the field of the camera, so as to increase the number of
time-space coordinates available for calculations of Mach number
and drag coefficients.

When the models are projected, they are guided the length of the
catapulting mechanism by means of a balsa cradle; this cradle quickly
separates from the model after the model leaves the catapulting
mechanism and is considered to have no effect on the subsequent motion
of the model.

For each test flight a quadratic equation of the form

$$t = c_0 + c_1 s + c_2 s^2$$

is fitted to the space-time coordinates, for all positions in which the
model is detected, by the conventional least-squares methods (refer-
ence 4).

The drag coefficient of the nose section in flight can be obtained
from the equation

$$C_D = \frac{2Wa}{g\rho AV^2}$$

where V is the first time derivative of s, and a is the second.
That is

$$V = \frac{1}{c_1 + 2c_2 s}$$

$$a = \frac{-2c_2}{(c_1 + 2c_2 s)^3}$$

Models

The models used during the investigation were scale models of
jettisonable nose sections typical of those being incorporated into the
design of current transonic and supersonic research aircraft. The
models were built and prepared for testing by the Langley Laboratory.
Eight models were built, four of each of the two nose designs considered
in this investigation. For each design two models were constructed
without stabilizing fins and two were constructed incorporating
stabilizing fins. The models of each nose design constructed without
fins will hereinafter be referred to as models 1 and 2 and the

corresponding designs with fins installed will be referred to as
models 3 and 4. The fins installed on models 3 and 4 were curved to
the contour of the nose section so that on a full-scale nose section
they might be retractable. The size fins used were those found
necessary to stabilize the nose sections at low speeds (reference 1).

Drawings of models 1, 2, 3, and 4 which represented each of the
two types of nose sections, both with and without stabilizing fins
installed, are presented in figures 1 to 4 and photographs of the
corresponding models are presented as figures 5 to 8. The scale of
the models tested varied from 1/19 to 1/10 depending upon the design
and upon whether fins were installed. The different scales were
selected so as to obtain models of the maximum size that could be
successfully projected in the Langley free-flight apparatus, larger
models generally enhancing the probability of obtaining film results.

As indicated in the section entitled "Analysis," the ratio of the
density of a full-scale section to the air must be the same as the
ratio of the density of a corresponding model to the air. The models
without fins installed were ballasted with lead weights to obtain
dynamic similarity to corresponding full-scale jettisonable nose sec-
tions at a desired test altitude of 15,000 feet. As indicated previ-
ously, the models on which fins were incorporated were smaller than
those without fins, and when these models were constructed, their
structural weight exceeded the desired weight for testing to correspond
to a full-scale design at an equivalent altitude of 15,000 feet.
Model 3 was ballasted to represent a corresponding nose section at an
equivalent test altitude of 50,000 feet and model 4 was ballasted for
an equivalent test altitude of 18,700 feet. This increased their
respective desired weights for testing to values high enough to permit
ballasting. The equivalent test altitude of model 3 was considerably
higher than that of the other models because of its extremely small
size and associated difficulties in distributing ballast. The weight
of the stabilizing fins was included in the desired weights of models 3
and 4. Table I is a presentation of the mass characteristics of the
models (given in terms of full-scale values).

Analysis

The equations used in converting model test results to those that
would be obtained with a corresponding full-scale nose are herewith
presented. Theories of dynamic similitude presented in reference 4
have been modified to apply to models when (1) the Mach number for
the model is equal to the Mach number for the full-scale nose section,
and (2) a small effect of gravity on the model for a short-time
period of model action is neglected.

As pointed out in reference 5, in order for dynamic similitude to exist between a model and a full-scale section, the ratio of the full-scale aerodynamic forces to the model aerodynamic forces must be equal to the ratio of the full-scale inertia forces to the model inertia forces, as indicated in the following equation:

$$\frac{F_{fs}}{F_m} = \frac{l_{fs}^2 V_{fs}^2}{l_m^2 V_m^2} \frac{\rho_{fs}}{\rho_m} = \frac{m_{fs} a_{fs}}{m_m a_m} \tag{1}$$

It should be noted that the term $\frac{\rho_{fs}}{\rho_m}$ was omitted in reference 5 because $\frac{\rho_{fs}}{\rho_m}$ was assumed to be equal to one. Inasmuch as $M_{fs} = M_m$, velocities obtained experimentally at sea level must be multiplied

by $K \left(\frac{\text{Velocity of sound at altitude}}{\text{Velocity of sound at sea level}} \right)$ in order to obtain velocities at test altitude. This correction is necessary because of the fact that the speed of sound at sea level is greater than the speed of sound obtained as the altitude is increased. Let $\frac{l_{fs}}{l_m} = R$. Substitution of $\frac{l_{fs}}{l_m} = R$ and $\frac{V_{fs}}{V_m} = K$ in equation (1) results in

$$R^2 K^2 \frac{\rho_{fs}}{\rho_m} = \frac{m_{fs} a_{fs}}{m_m a_m}$$

or

$$\frac{a_{fs}}{a_m} = \frac{m_m}{m_{fs}} R^2 K^2 \frac{\rho_{fs}}{\rho_m} \tag{2}$$

In order to determine the relationship for acceleration between the model and the corresponding full-scale section from equation (2), it is necessary to determine the relationship existing between the corresponding mass terms.

As indicated in reference 5, in order that both model and full-scale section have similar motion, they must have similar helix angles. That is

$$\frac{\omega_{fs} l_{fs}}{V_{fs}} = \frac{\omega_m l_m}{V_m} \tag{3}$$

Then, since $\dfrac{V_{fs}}{V_m} = K$ and $\dfrac{l_{fs}}{l_m} = R$,

$$\omega_{fs} = \frac{\omega_m K}{R} \tag{4}$$

Since centripetal acceleration is $\omega^2 l$

$$\frac{l_{fs}^2 V_{fs}^2 \rho_{fs}}{l_m^2 V_m^2 \rho_m} = \frac{m_{fs}\omega_{fs}^2 l_{fs}}{m_m \omega_m^2 l_m} \tag{5}$$

Then

$$\frac{m_{fs}}{m_m} = R^3 \frac{\rho_{fs}}{\rho_m} \tag{6}$$

It can be seen that equation (6) expresses the necessary condition that the ratio of the density of a full-scale section to that of air equals the ratio of the density of the corresponding model to that of air, since

$$\frac{m_{fs}}{\rho_{fs} l_{fs}^3} = \frac{m_m}{\rho_m l_m^3}$$

or

$$\frac{m_{fs}}{m_m} = R^3 \frac{\rho_{fs}}{\rho_m}$$

Substituting for the mass term in equation (2):

$$a_{fs} = \frac{a_m K^2}{R} \tag{7}$$

Similarly, other relations are:

$$t_{fs} = t_m \frac{R}{K}$$

$$I_{fs} = I_m R^5 \frac{\rho_{fs}}{\rho_m}$$

RESULTS AND DISCUSSION

As mentioned previously, two models were built of each design and configuration. Both sets of results are presented for model 1, the second set being referred to as results for model 1a. Only one set of results was obtained for model 2 and for model 4 because the alternate firings of these models were unsuccessful. Two sets of results were obtained for model 3 but because of their similarity only one set is presented herein.

The results of the present investigation are presented in figures 9 to 14 in the form of photographs of the models in flight taken at various stations along their flight path. Table II is a presentation of measurements accurately locating the model in each picture, a timing record, and results of calculations made to determine the Mach number at the points at which the photographs of figures 9 to 14 were obtained. The letter "a" adjacent to each station number on table II indicates the first exposure on each film, and "b" the second exposure (if one were obtained). These measurements and calculations are believed to be accurate to 1 percent.

Figures 9 and 10 indicate that models 1 and 1a, which were identically similar and had no stabilizing fins, were unstable. Model 1 pitched up when projected and model 1a pitched down when projected; the rate of pitch of the models appeared to be practically the same in each case. Calculations made for model 1 to determine the largest accelerations which would act on a pilot during the flight of a corresponding airplane nose indicate that due to the pitching motion which between stations 4b and 6a was approximately a 63° rotation (from 12° to 75° incidence) in a period of time of 0.135 second (full-scale at 15,000 ft altitude) there would occur a full-scale centripetal acceleration q^2r of approximately 4.3g. The component of this acceleration acting along the backbone of the pilot would be approximately 3.3g. Between stations 6a and 6b, the nose pointed up approximately 75° to the direction of flight and, due to the associated drag rise, the linear acceleration acting along the backbone of the pilot in a corresponding airplane nose at an altitude of 15,000 feet would be 12.1g for 0.014 second. For the case (model 1) in which the nose turned up, the corresponding acceleration on a pilot sitting erect would be positive and could probably be withstood. If, however, it noses down as it did for model 1a, the acceleration would be negative. Reference 6 indicates the possible danger of such a negative acceleration although it has been indicated that recent experience by the Air Force points to the possibility that man's tolerence of negative acceleration may be greater than the limits shown in reference 6. The time history of the forward movement of model 1a appeared to be generally similar to that of model 1 and is not presented in tabular form.

When model 2, the other nose section without fins, was projected in the Langley free-flight apparatus, it too turned away from a nose-first flight attitude (fig. 11). Calculations indicated that although the centripetal acceleration due to rotation of a corresponding full-scale nose section would not be large, the deceleration along the flight path associated with the drag rise when the nose turned away from a nose-first attitude would again be large. For example, between stations 4a and 4b the nose pointed down approximately 90° to the flight path, and a pilot in a corresponding full-scale nose section at 15,000 feet altitude would undergo a high negative acceleration of 26.4g for a period of time of 0.013 seconds. It can be observed in figure 11 that model 2 started to disintegrate at station 5, probably because of faulty model construction.

When models 3 and 4, the fin-stabilized versions of models 1 and 2, respectively, were projected in the Langley free-flight apparatus, they were quite stable in flight as indicated by figures 12 to 14. Figure 13 is a shadowgraph of model 3 in flight and shows the flow pattern around the stabilized nose. The acceleration a pilot would receive in a stable full-scale nose section would act transversely where the human tolerance to acceleration is greatest. Calculations indicated that the corresponding motion in the full-scale nose section would not subject the pilot to large accelerations (approx. 3.5g full-scale for model 3 and approx. 5.9g full-scale for model 4 based on stations midway in the free-flight apparatus). It is felt that the rather large descent of model 4 in flight as compared with model 3 was caused by the fact that one or more of the fins of model 4 may have been damaged in launching. The drag coefficient obtained for model 3 was 0.943 at a Mach number of 1.199 and for model 4 the drag coefficient obtained was 0.603 at a Mach number of 1.177. Calculations of drag coefficient were not made for the unstable nose sections because an accurate enough time and angular displacement history of the rotation of the nose was not obtained to permit accurate calculations.

CONCLUSIONS

The results of the present investigation in which scale models of jettisonable nose sections of current research aircraft were projected at supersonic speeds in the Langley free-flight apparatus indicate that unstabilized nose sections will turn away from a nose-first flight attitude, and calculations indicate that a pilot within a corresponding full-scale nose section may encounter large accelerations as a result of this instability. When nose sections are stabilized with fins, they will continue in a stable nose-first attitude and calculations have

indicated that the corresponding motion in the full-scale nose section would not subject the pilot to large accelerations.

Langley Aeronautical Laboratory
    National Advisory Committee for Aeronautics
        Langley Air Force Base, Va.

<div align="center">REFERENCES</div>

1. Scher, Stanley H.: An Empirical Criterion for Fin Stabilizing
      Jettisonable Nose Sections of Airplanes. NACA RM L9I28, 1949.

2. Scher, Stanley H., and Gale, Lawrence J.: Motion of a Transonic
      Airplane Nose Section When Jettisoned As Determined from Wind-
      Tunnel Investigations on a $\frac{1}{25}$-Scale Model. NACA RM L9L08a, 1950.

3. Goodwin, Roscoe H.: Wind-Tunnel Investigation at Low Speed to
      Determine Aerodynamic Properties of a Jettisonable Nose
      Section with a Circular Cross Section. NACA RM L9J13, 1950.

4. Crout, Prescott D.: A Short Method for Evaluating Determinants
      and Solving Systems of Linear Equations with Real or Complex
      Coefficients. Trans. AIEE, vol. 60, 1941, pp. 1235-1240.

5. Scherberg, Max, and Rhode, R. V.: Mass Distribution and Performance
      of Free Flight Models. NACA TN 268, 1927.

6. Lombard, Charles F.: How Much Force Can Body Withstand? Aviation
      Week, vol. 50, no. 3, Jan. 17, 1949, pp. 20-28.

TABLE I.- MASS CHARACTERISTICS AND EQUIVALENT TEST ALTITUDE OF

MODELS OF JETTISONABLE NOSE SECTIONS INVESTIGATED IN THE

LANGLEY FREE-FLIGHT APPARATUS

[Model values converted to corresponding full-scale values; moments of inertia are given about center of gravity]

Model	Weight (lb)	Moments of inertia $(slug\text{-}ft^2)$			Equivalent altitude at which tested (ft)
		I_X	I_Y	I_Z	
1	727	27.1	81.2	71.7	15,000
2	977	24.1	129.3	126.0	15,000
3	1019	48.8	60.7	60.7	50,000
4	1062	55.4	182.7	185.5	18,700

NACA
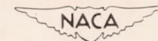
TABLE II.- PERTINENT DATA OF THE FLIGHT OF MODELS OF JETTISONABLE

NOSE SECTIONS INVESTIGATED IN THE LANGLEY FREE-FLIGHT APPARATUS

[All values are model values at sea level.]

Station	Displacement of nose point from end of catapulting mechanism (ft)	Time (sec)	Mach number	Photographs presented in figure
Model 1				
1a	8.731	0.0000	1.347	
1b	11.905	.0022	1.332	
2b	21.226	.0085	1.290	
4a	40.116	.0219	1.213	9
4b	41.689	.0231	1.207	
5a	50.715	.0299	1.173	
6a	58.165	.0359	1.147	
6b	59.684	.0372	1.141	

Speed of sound during test, 1115 ft per sec.

Model 2				
1a	8.902	.0000	1.418	
1b	12.148	.0021	1.381	
2a	20.356	.0077	1.297	
2b	21.376	.0084	1.281	11
4a	39.981	.0217	1.132	
4b	41.365	.0228	1.122	
5a	49.433	.0296	1.067	
5b	50.381	.0303	1.060	

Speed of sound during test, 1134 ft per sec.

Model 3				
1a	8.366	.0000	1.237	
1b	11.454	.0022	1.231	12
2a	20.105	.0085	1.214	
2b	20.649	.0091	1.212	
Shadowgraph	23.958	.0113	1.207	13
3a	28.428	.0146	1.199	
4a	39.969	.0231	1.178	
4b	41.661	.0244	1.175	12
5a	47.949	.0291	1.164	
5b	51.169	.0312	1.159	

Speed of sound during test, 1132 ft per sec.

Model 4				
1a	8.564	.0000	1.227	
1b	11.620	.0022	1.220	
2a	20.179	.0085	1.200	
3a	28.472	.0147	1.182	
3b	30.703	.0164	1.177	14
4a	37.719	.0217	1.161	
4b	41.095	.0242	1.154	
7a	71.854	.0486	1.093	

Speed of sound during test, 1127 ft per sec.
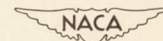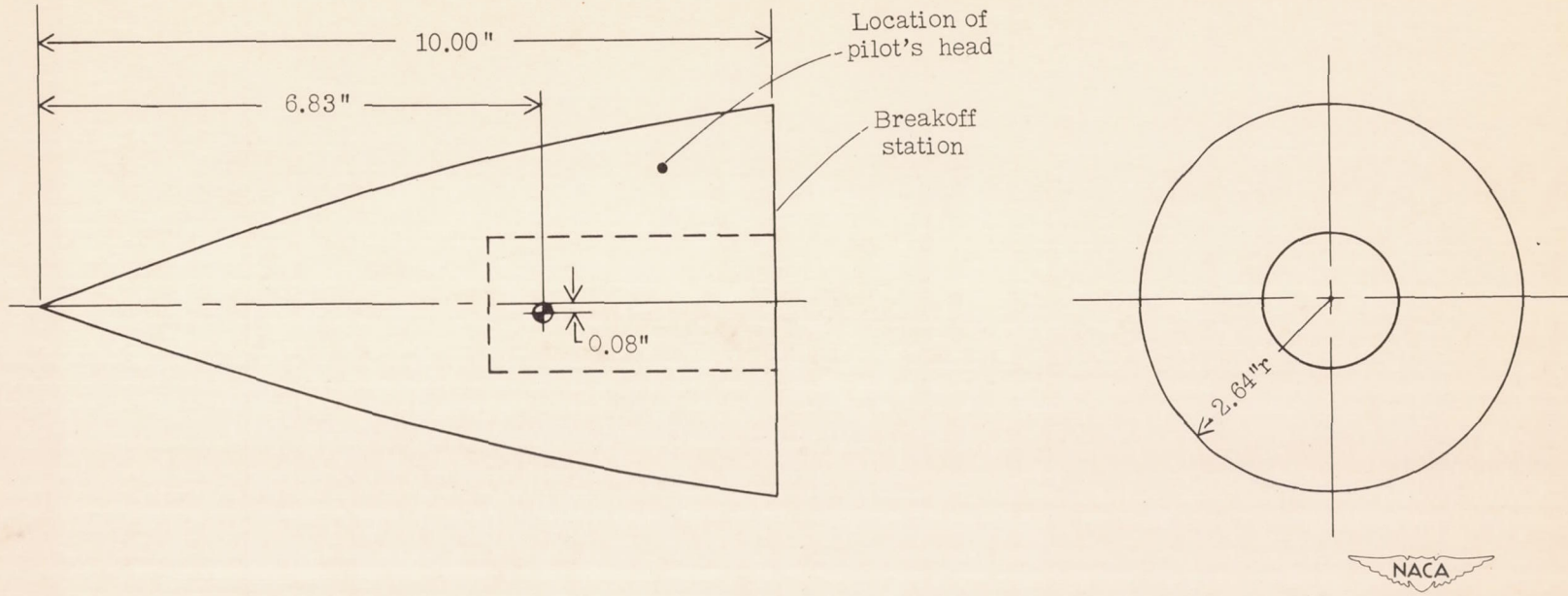
Figure 1.- Drawing of $\frac{1}{10}$-scale model 1. (Pilot's head in a corresponding full-scale nose section located 1.34 ft aft and 1.60 ft above center of gravity.)
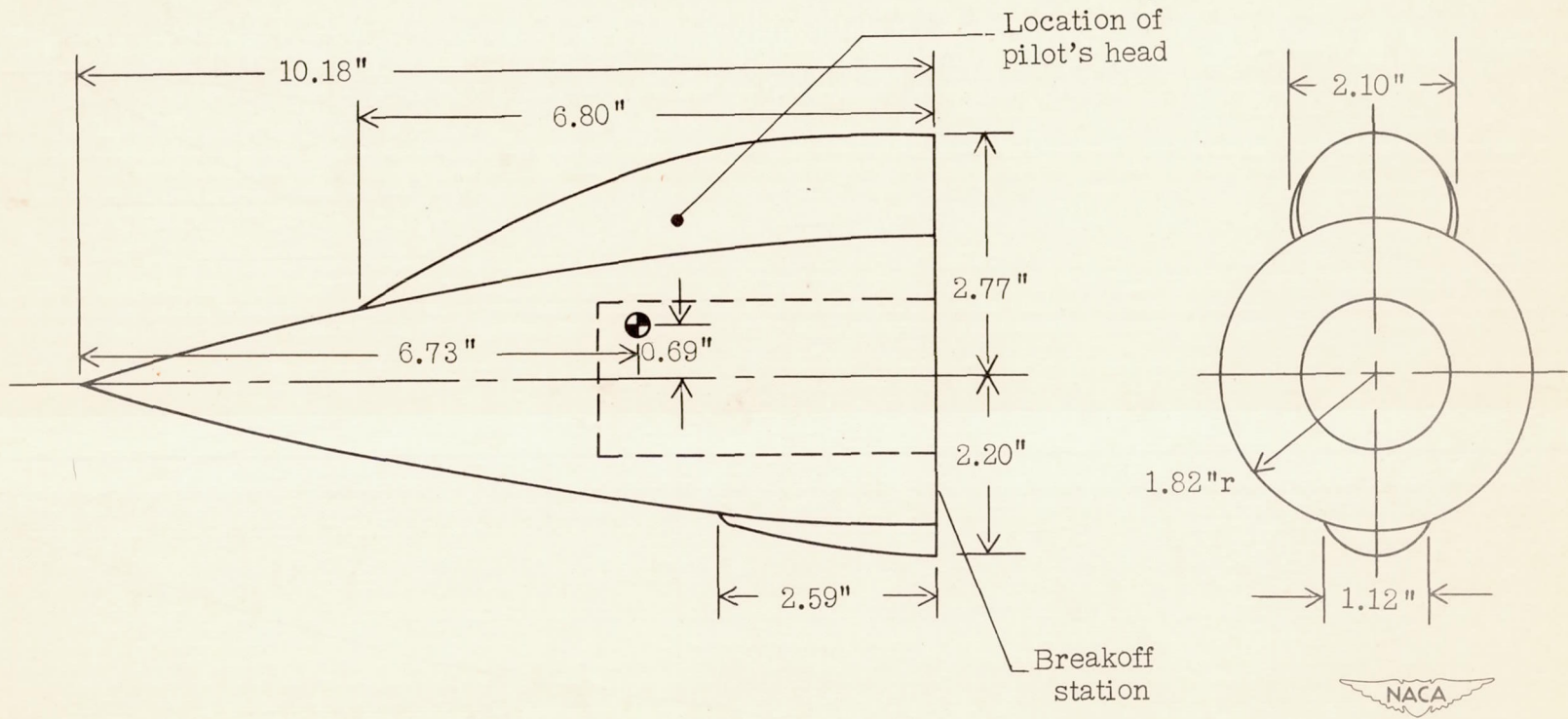
Figure 2.- Drawing of $\frac{1}{11}$-scale model 2. (Pilot's head in a corresponding full-scale nose section located 0.51 ft aft and 1.08 ft above center of gravity.)

5.26"

3.81"

Location of
pilot's head

Breakoff
station

0.01"

3.10"

0.79"

3°

0.85"

1.04"

1.18"

1.26"

1.07"

0.15"

Breakoff station

Sketch of fin

1.39" r

NACA
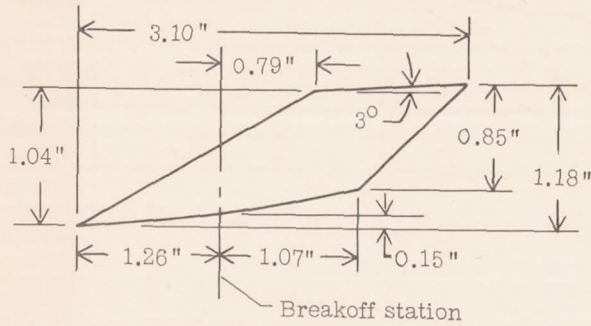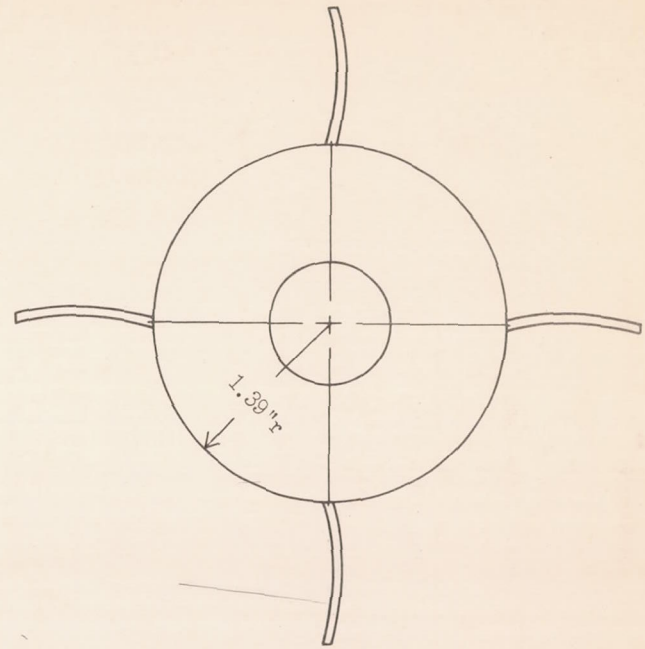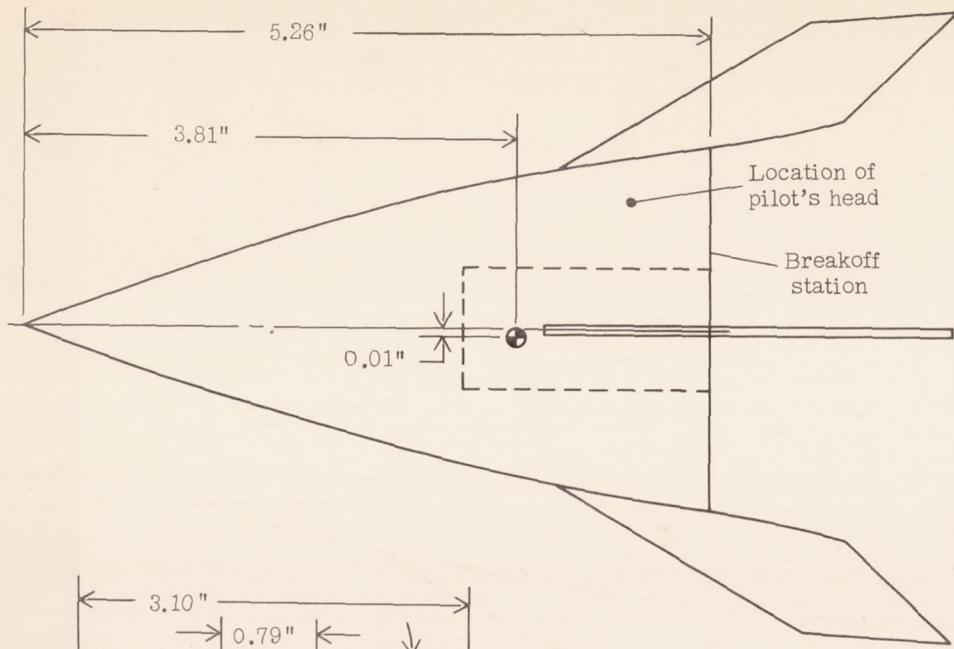
Figure 3.- Drawing of $\frac{1}{19}$-scale model 3.

Location of
pilot's head

7.47 "

5.22 "

2.03"

Breakoff
station

0.21"

1.62"

1.44 "

55° 55°

1.34"r

0.82"

NACA

0.4"   3.5 "

0.06"   1.14 "   1.2 "

1.9 "   2.0 "

3.9 "

Breakoff
station

Sketch of fin
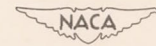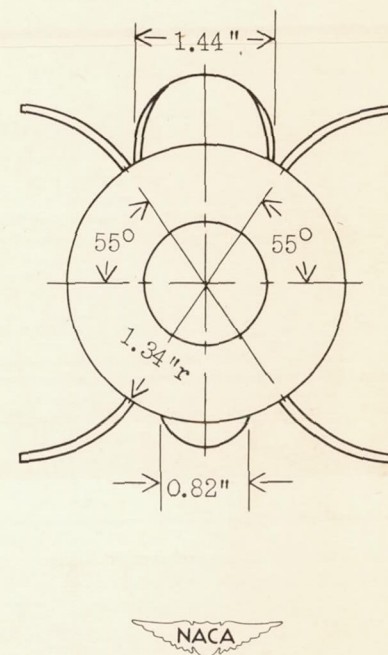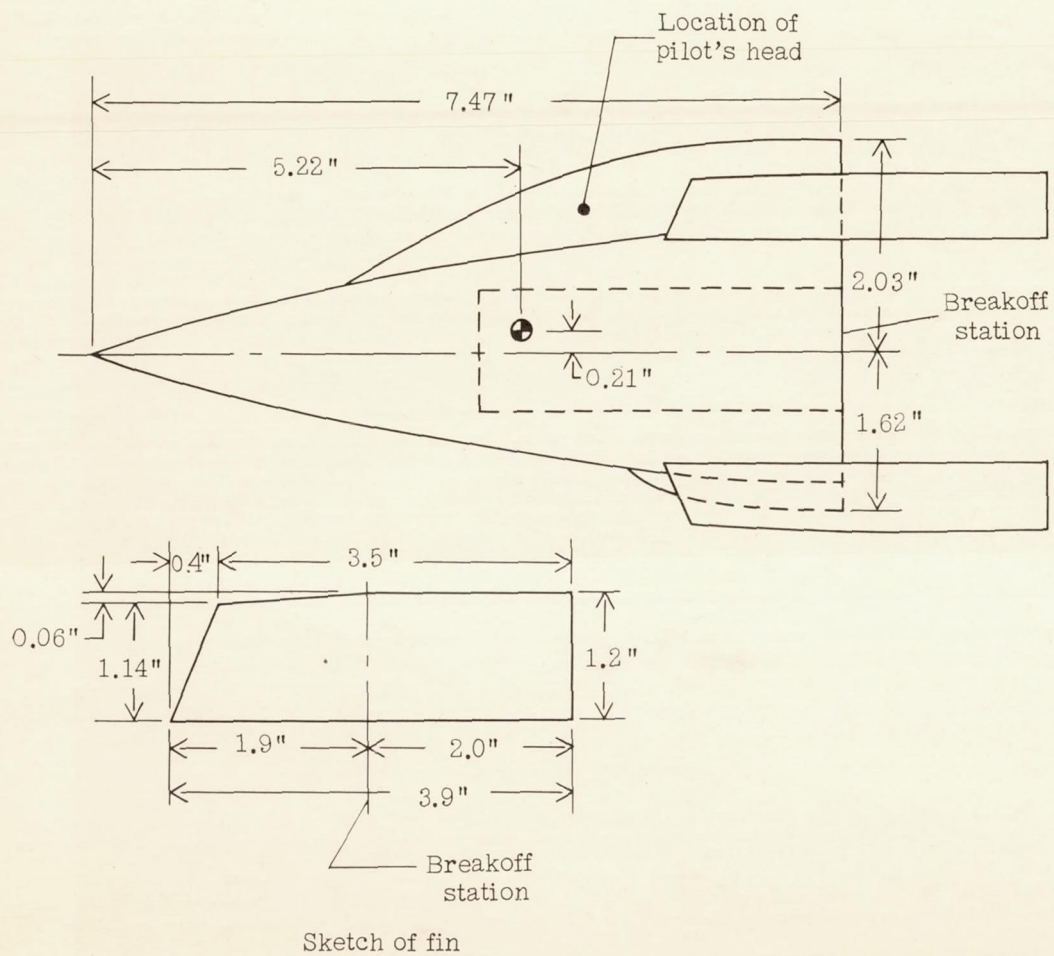
Figure 4.- Drawing of $\frac{1}{15}$-scale model 4.
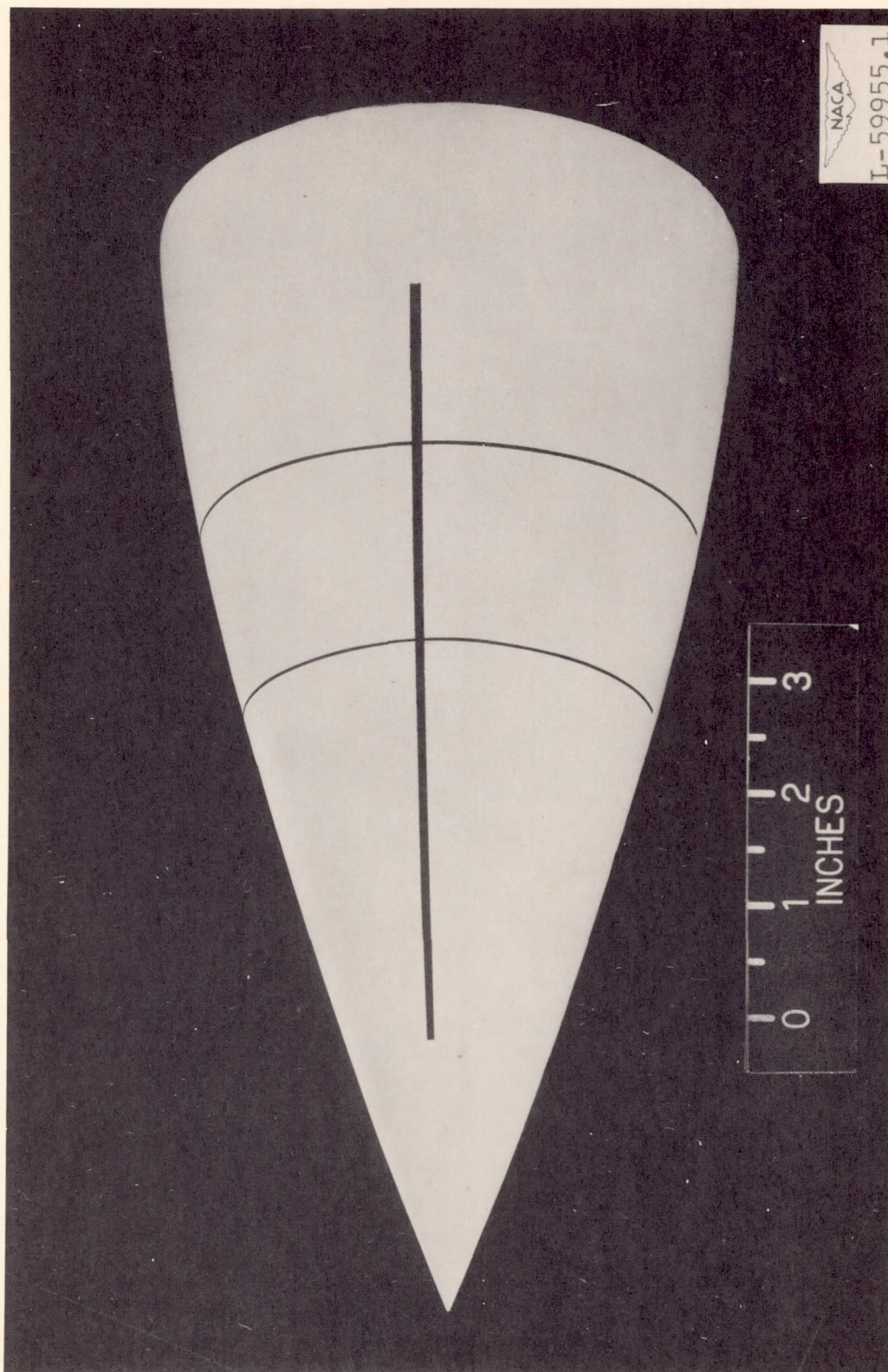
Figure 5.- Photograph of model 1.
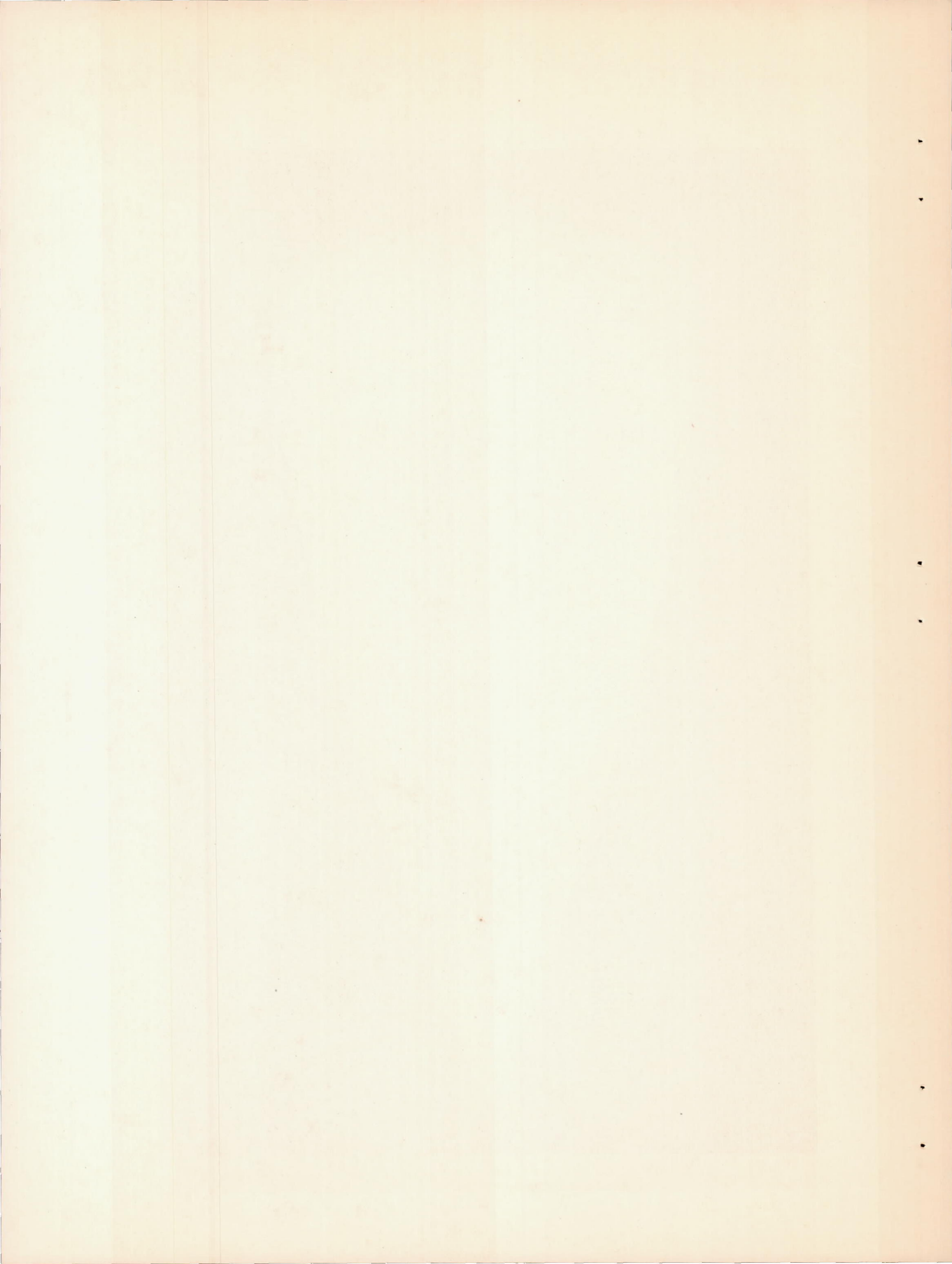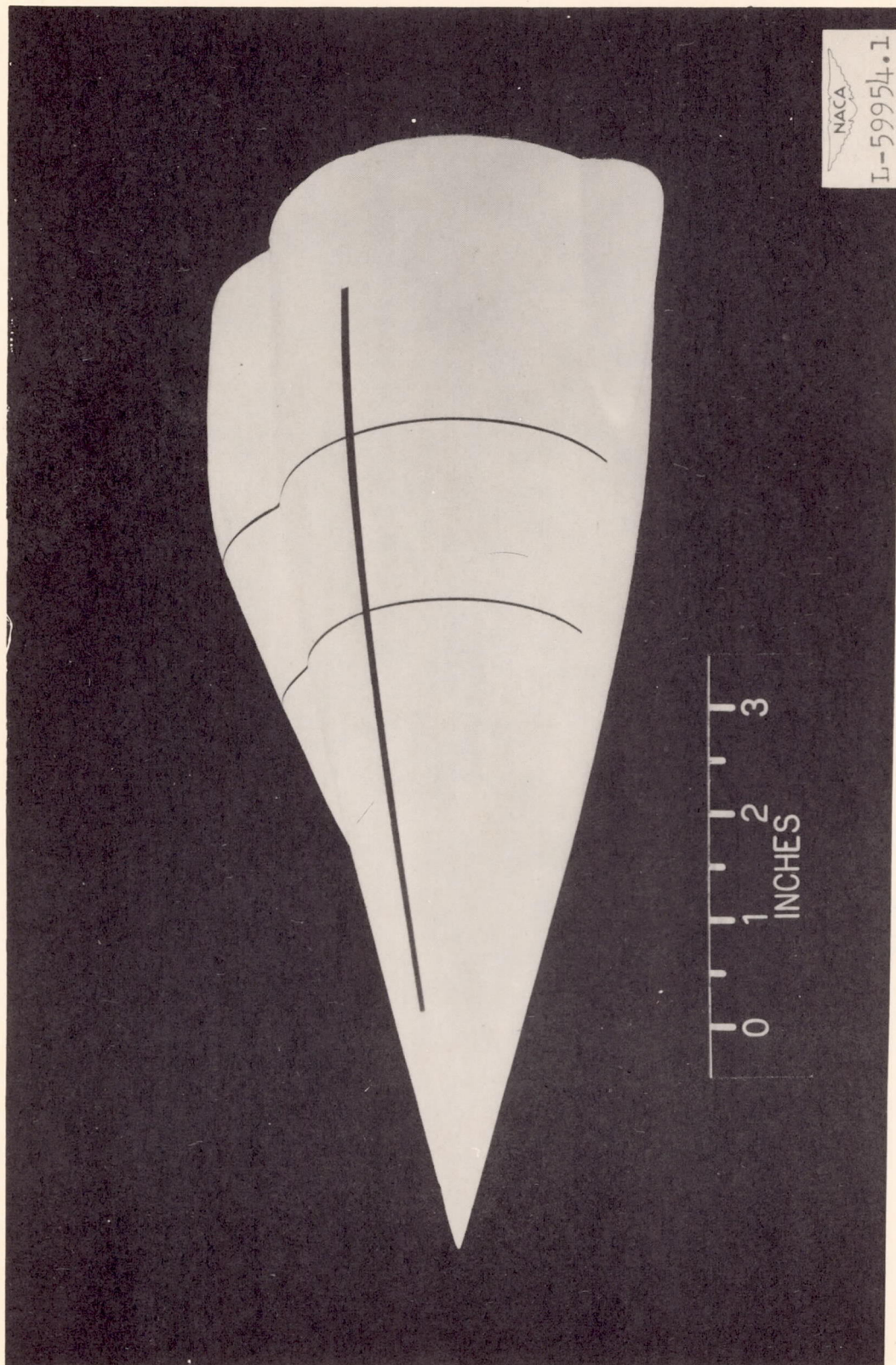
Figure 6.- Photograph of model 2.
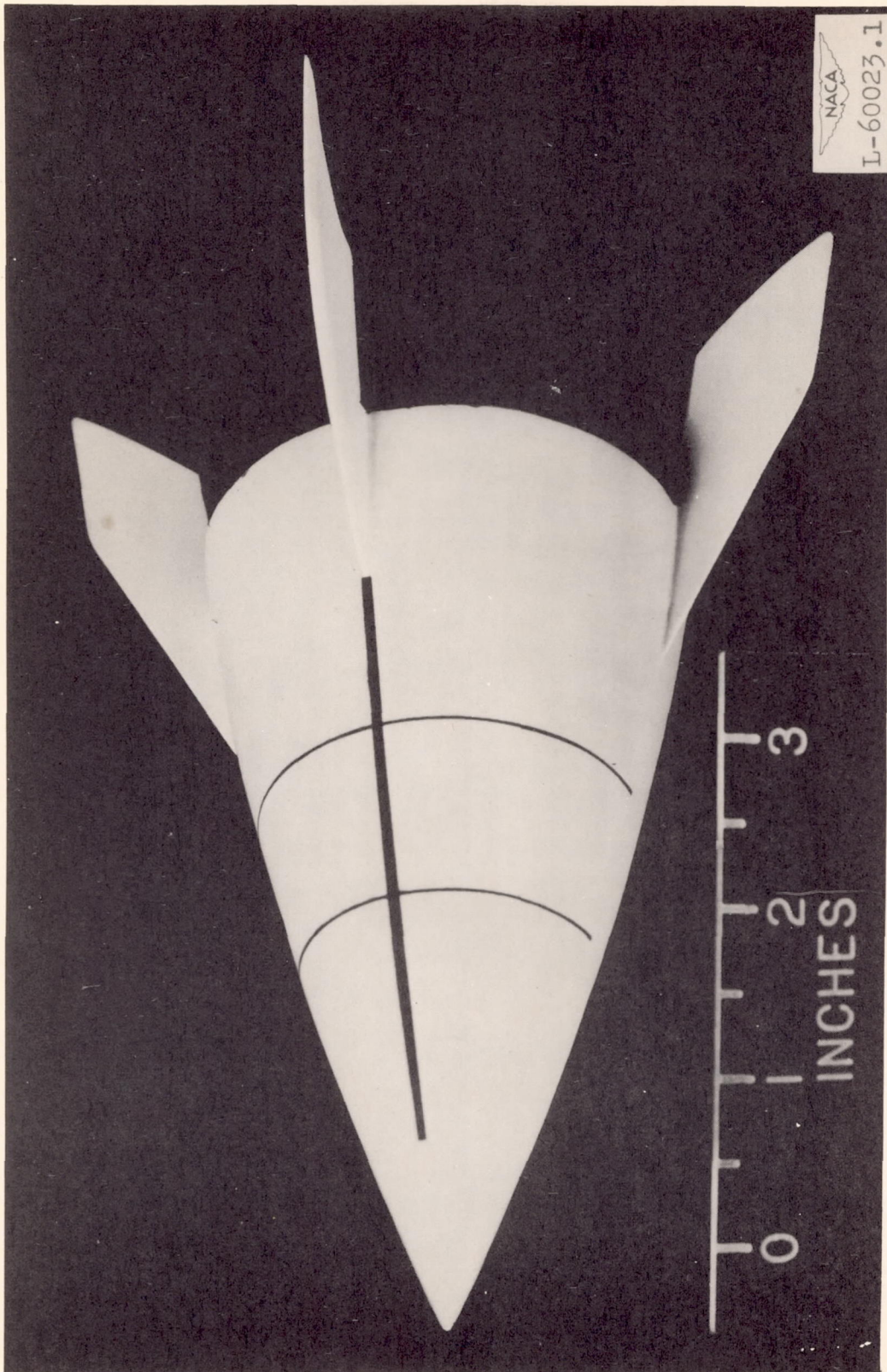
Figure 7.- Photograph of model 3.
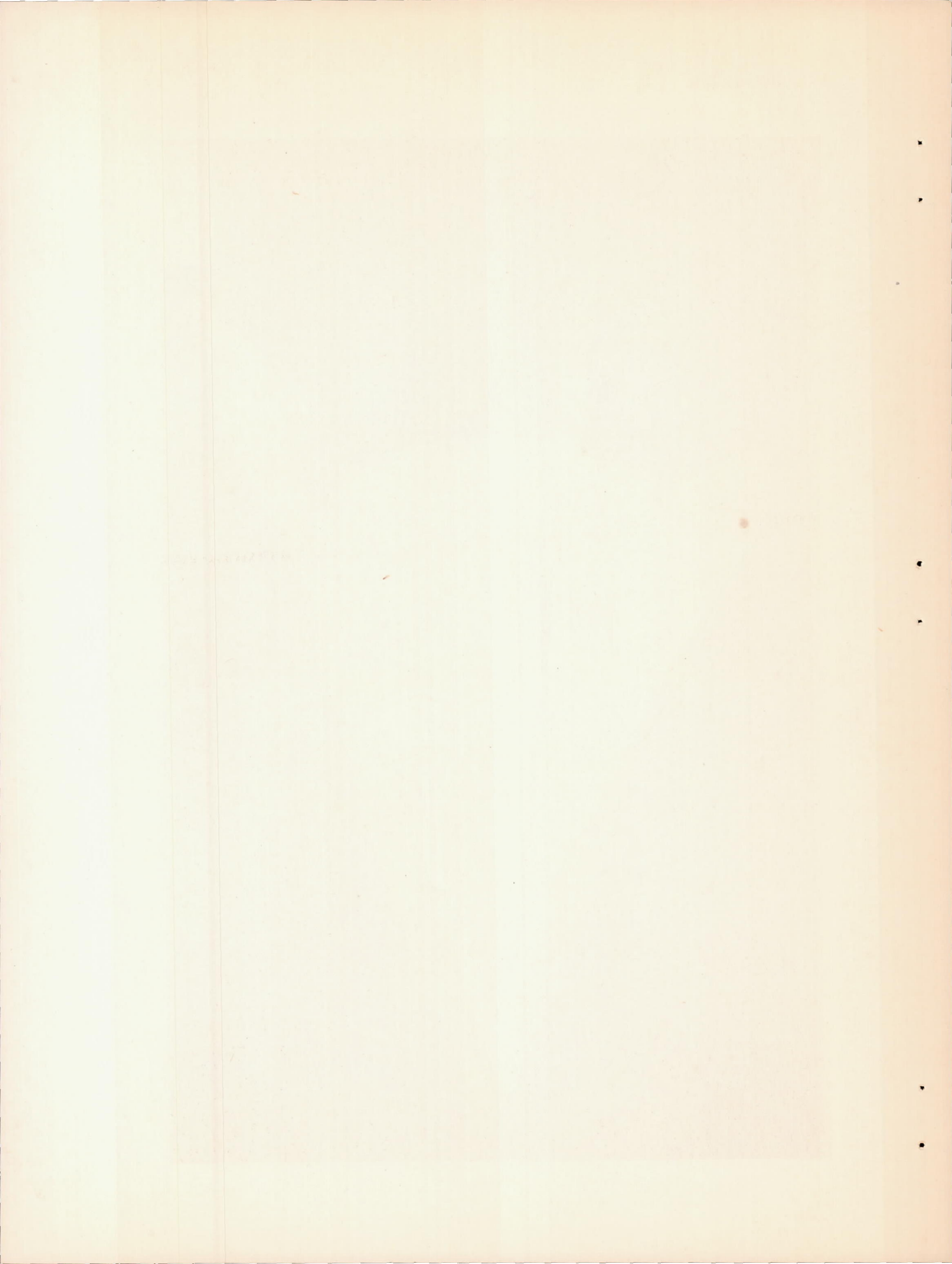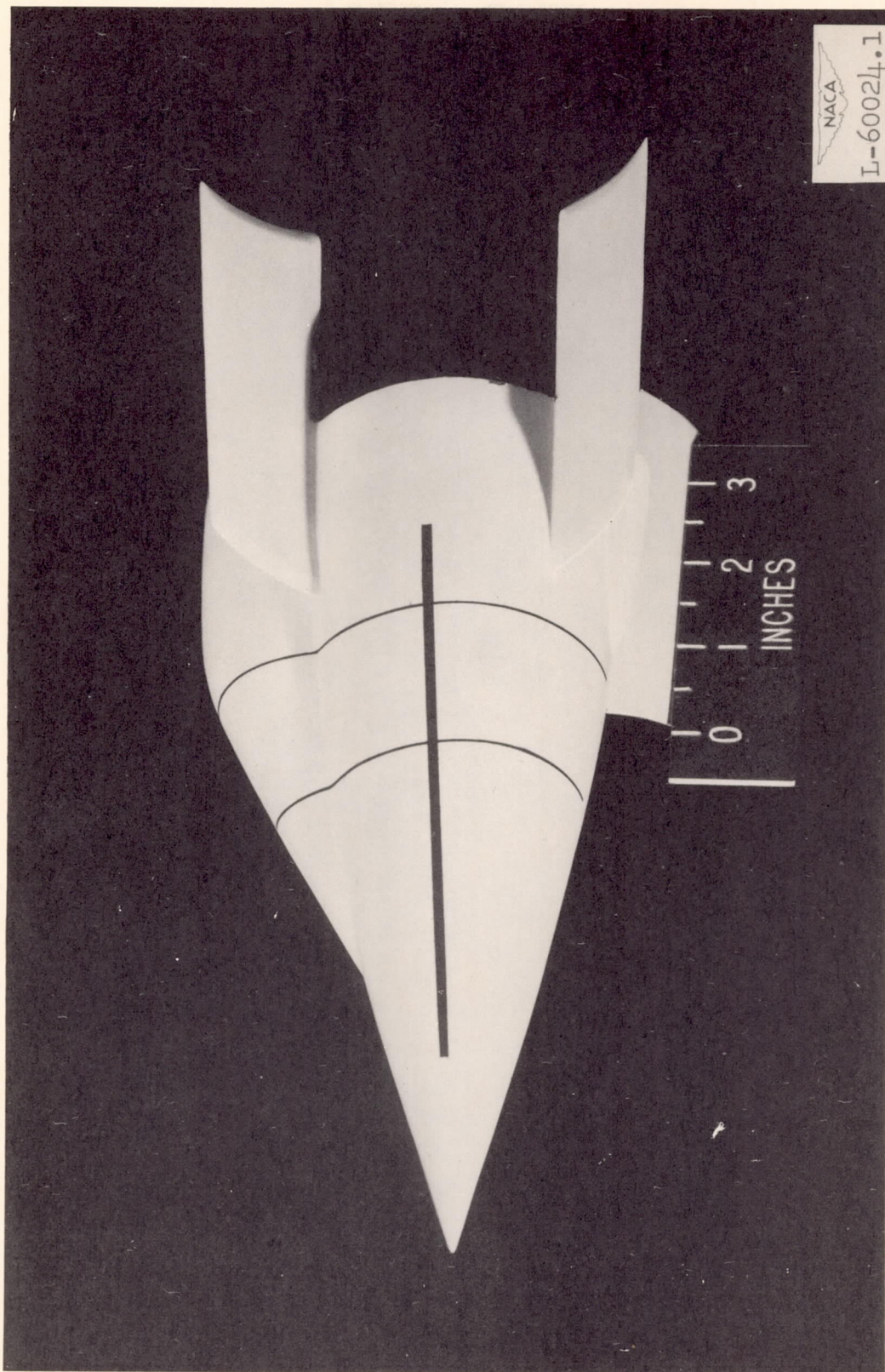
Figure 8.- Photograph of model 4.
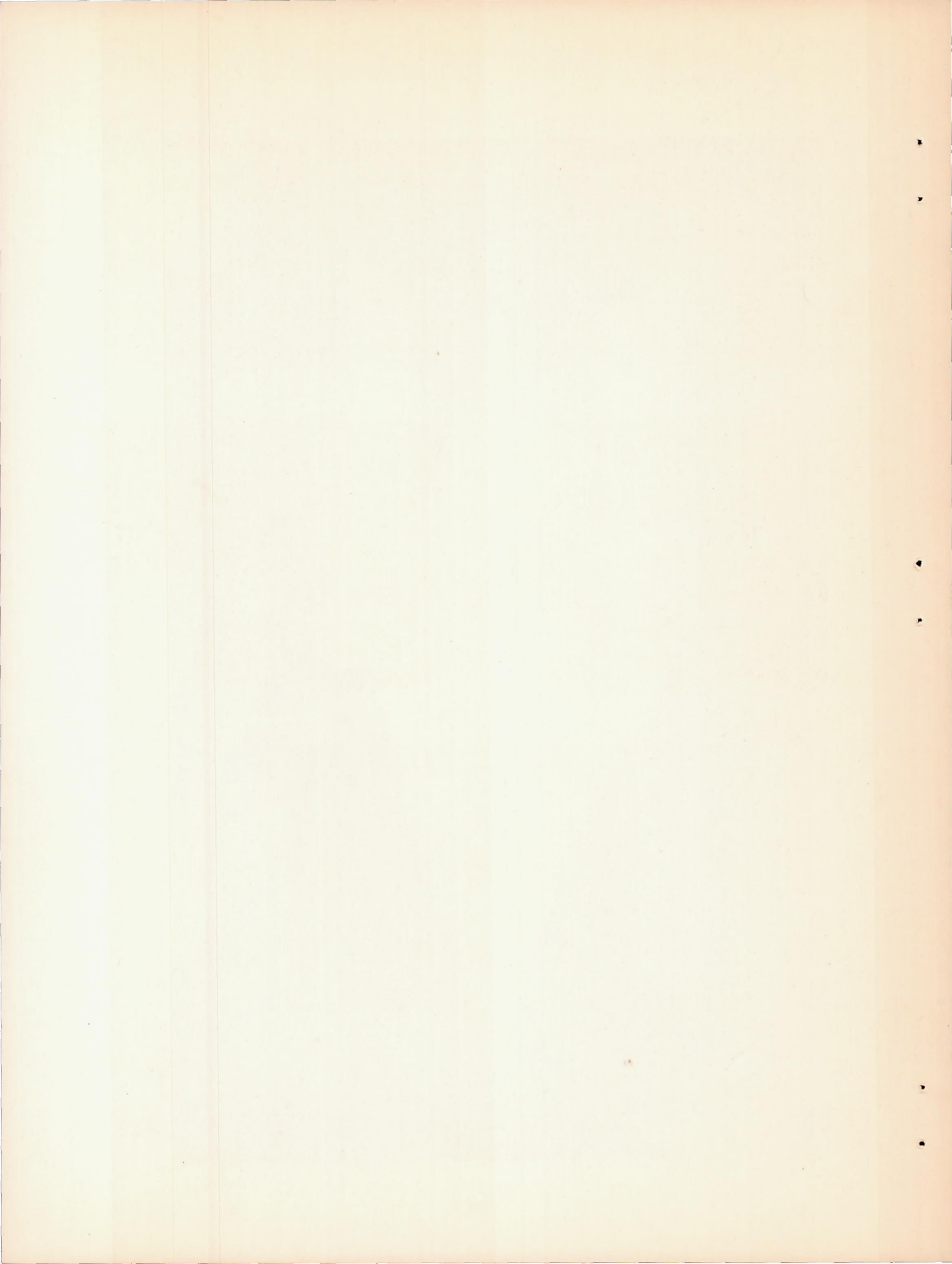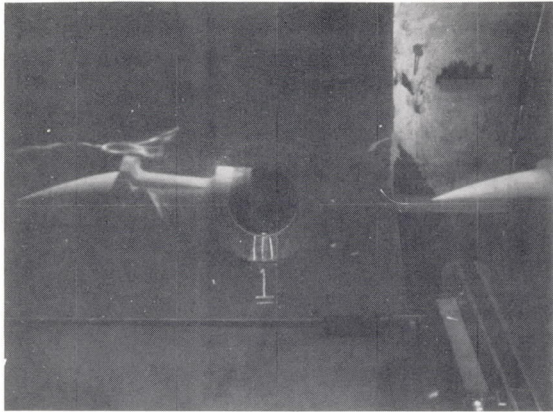
Station 1
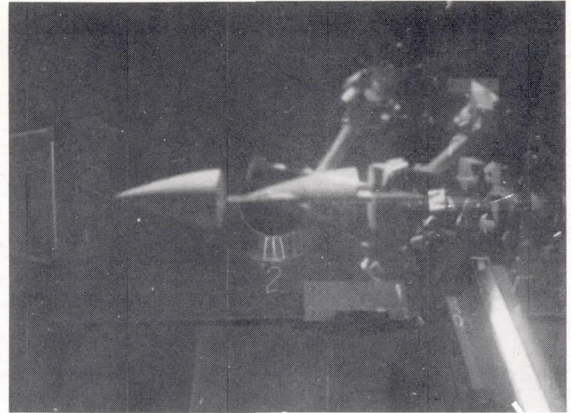
Station 2
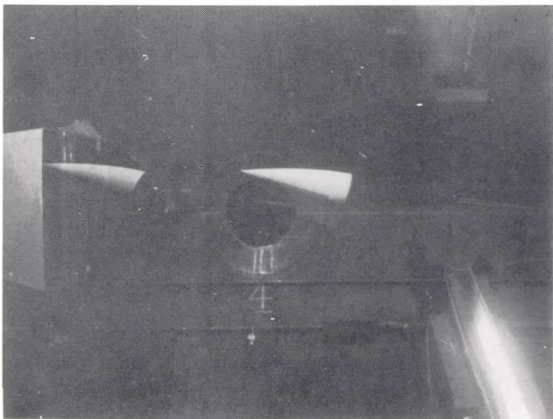
Station 4

Station 5
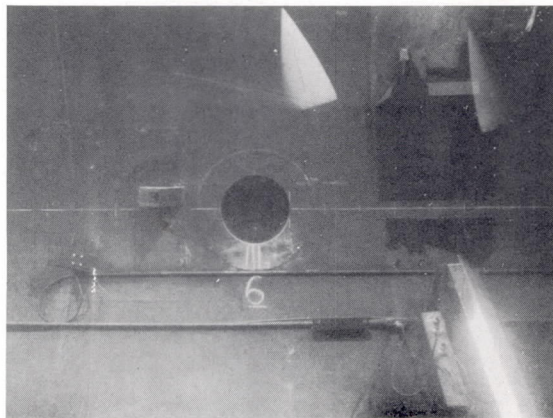
Station 6

L-63041

Direction of travel

Figure 9.- Motion of model 1 when projected at supersonic speeds in the
Langley free-flight apparatus. (Camera at station 3 failed.)
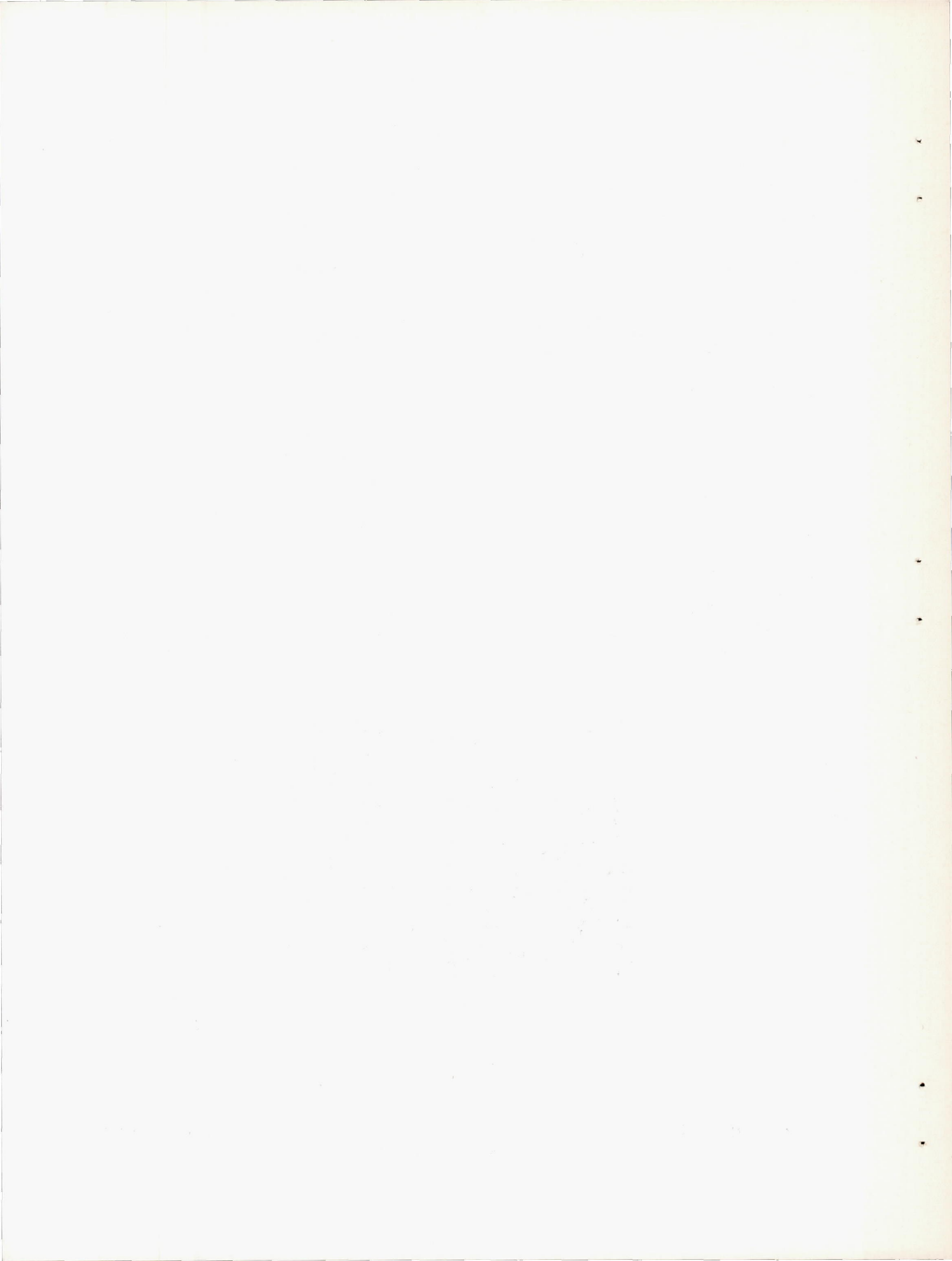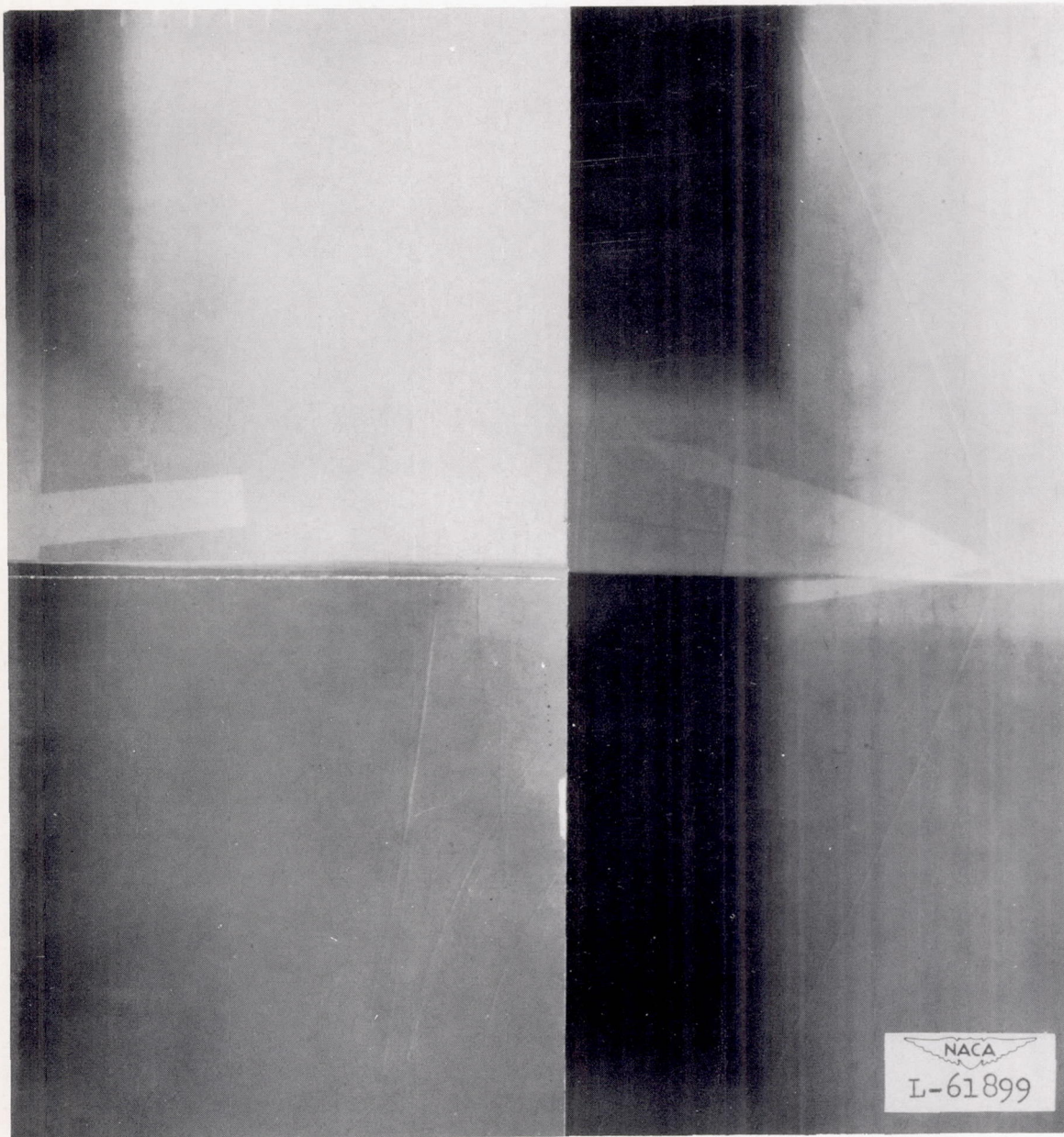
Station 1

Station 2

Station 3

Station 4

Station 5

L-63042

Direction of travel

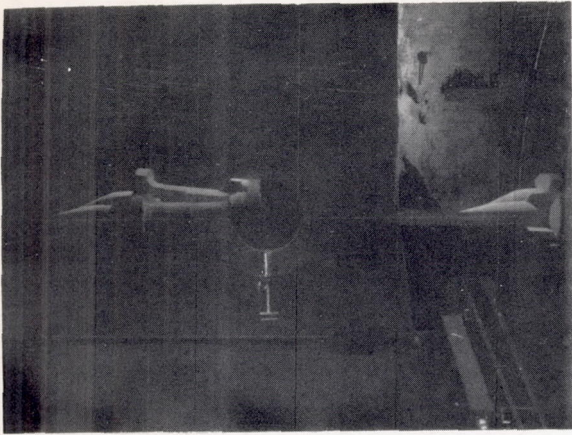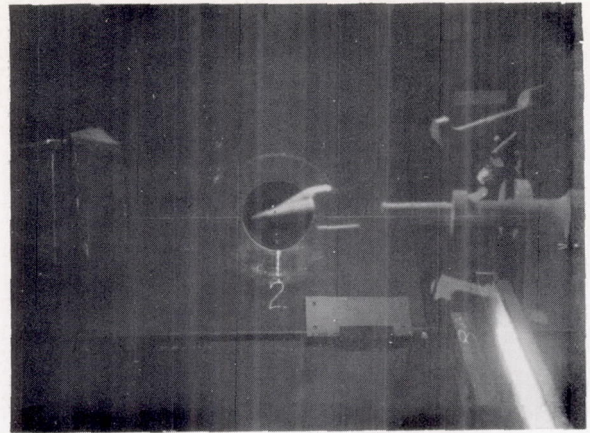Figure 10.- Motion of model 1a when projected at supersonic speeds in the Langley free-flight apparatus.

Station 1

Station 2

Base of model
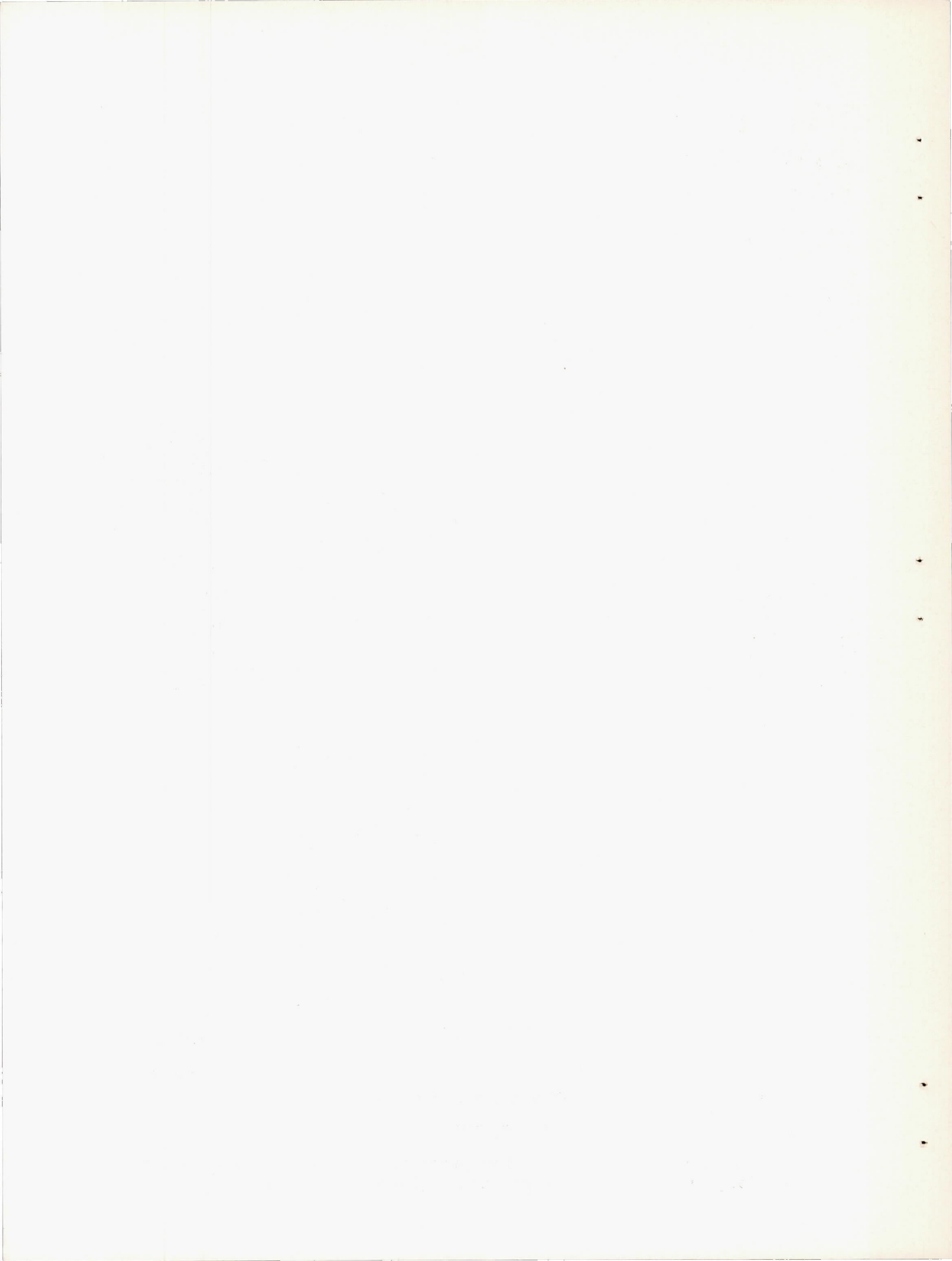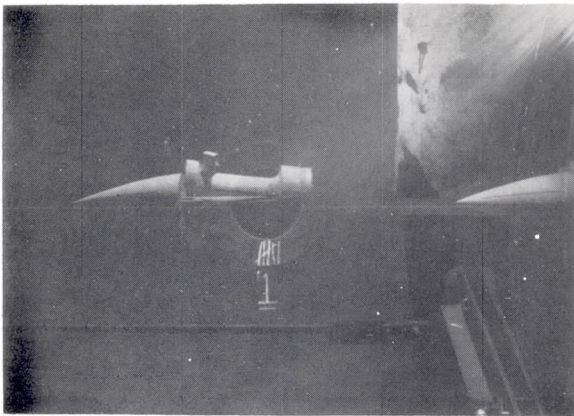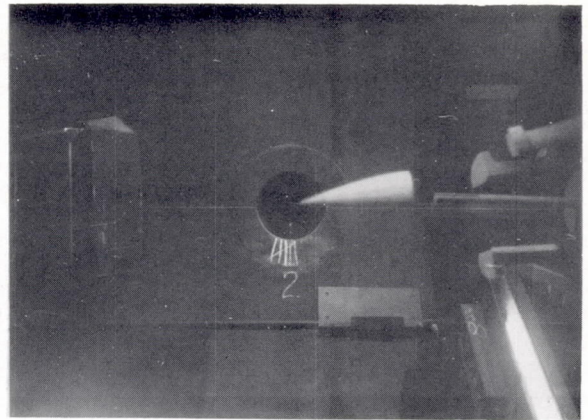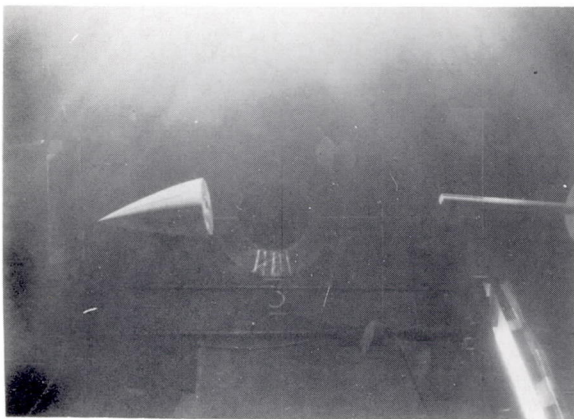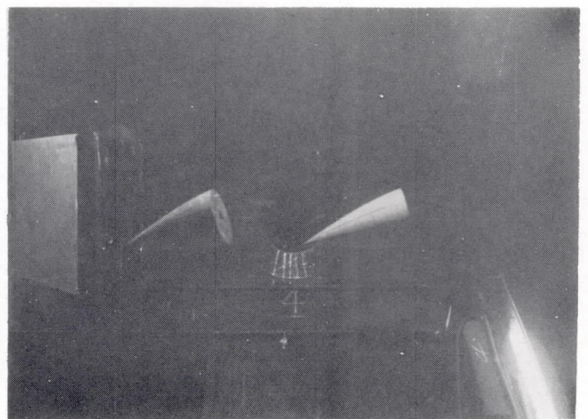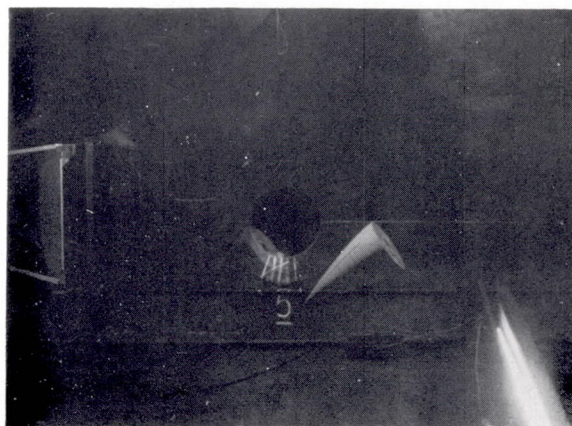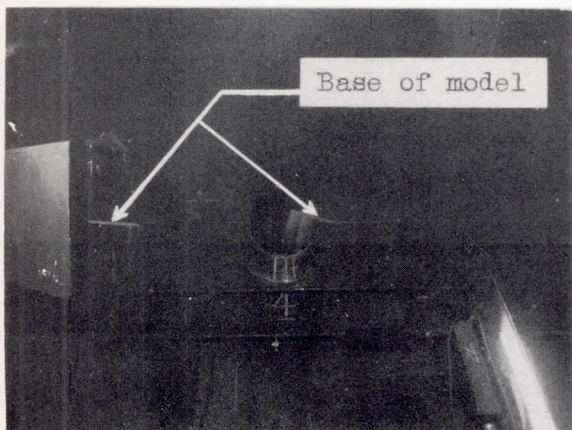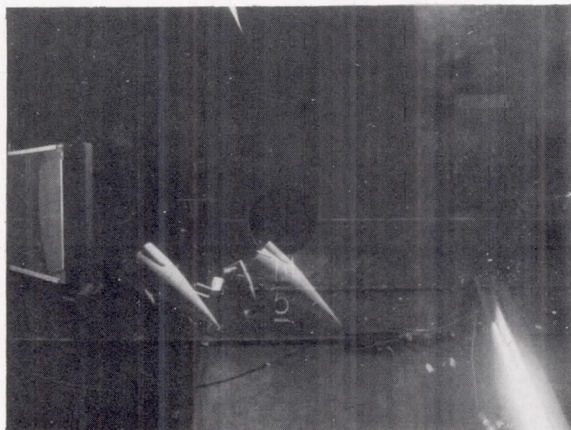
Station 4

Station 5

Direction of travel

NACA
L-63043

Figure 11.- Motion of model 2 when projected at supersonic speeds in the
Langley free-flight apparatus. (Camera at station 3 failed.)
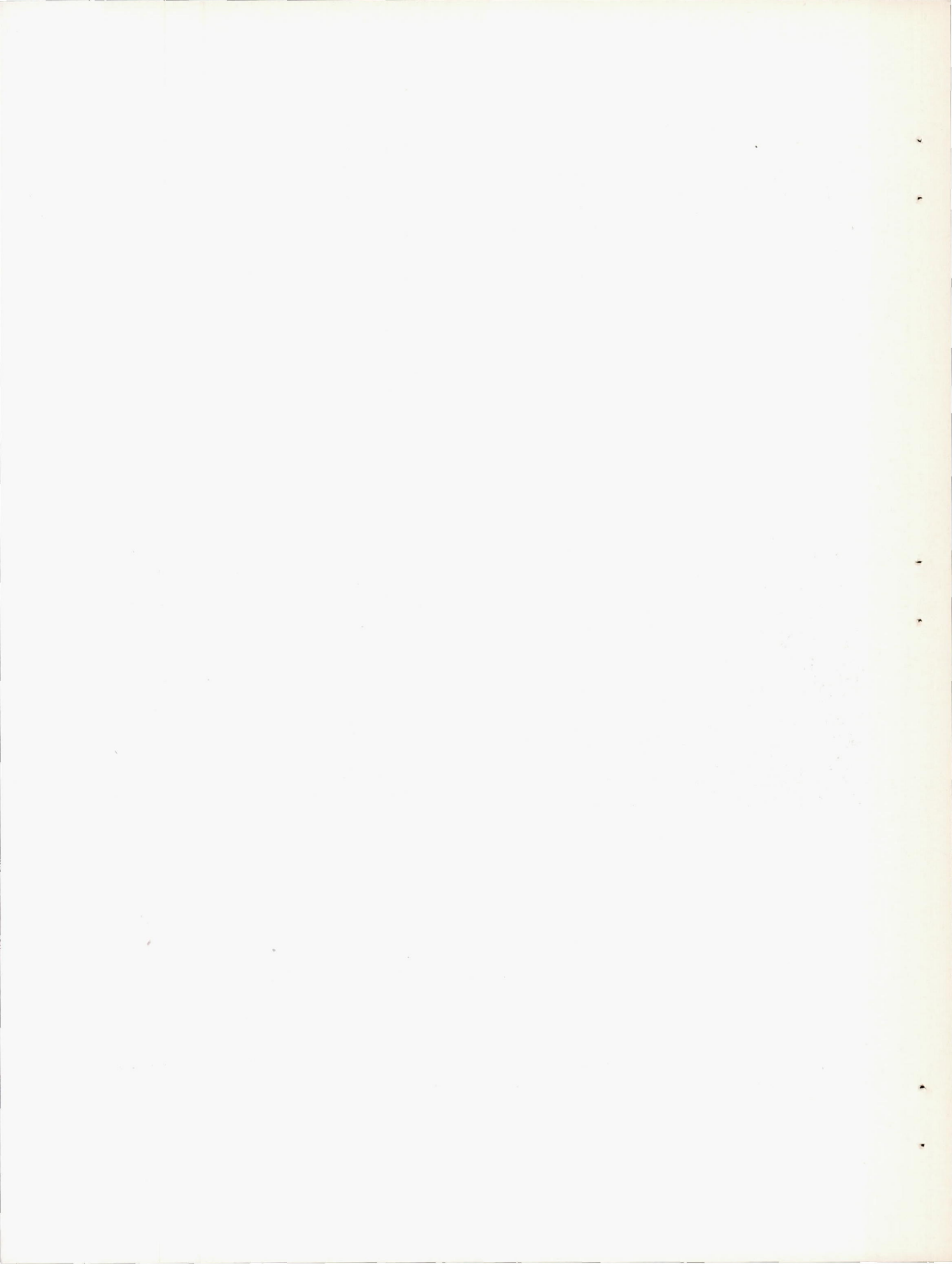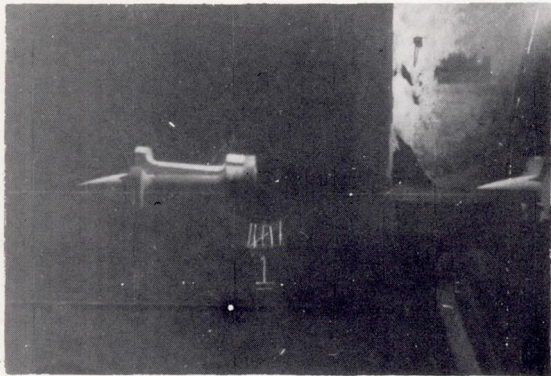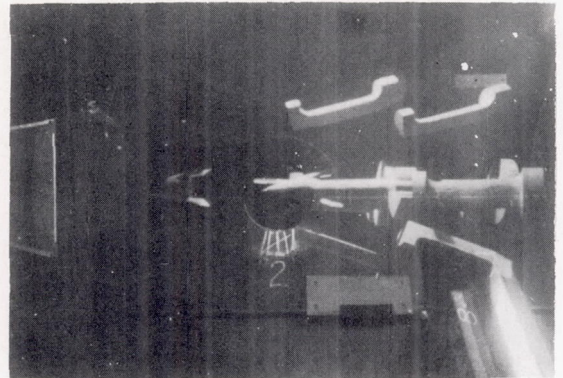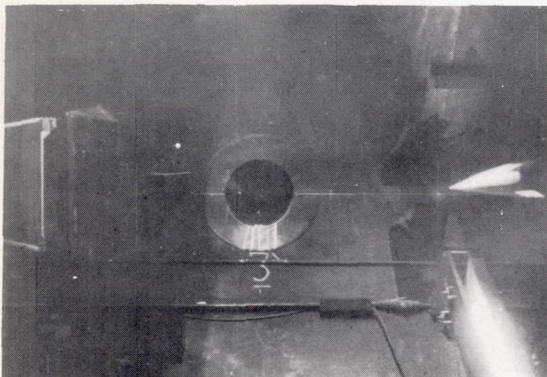
Station 1
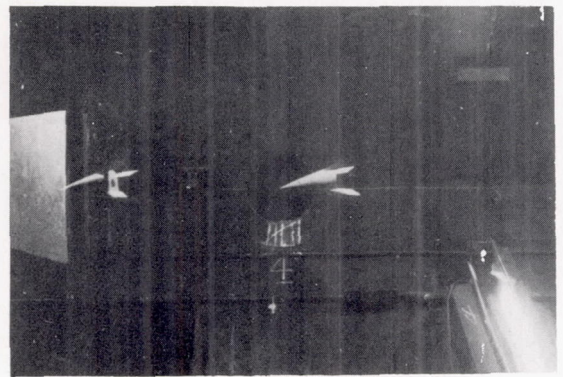
Station 2

Station 3

Station 4

Station 5

L-63044

Direction of travel

Figure 12.- Motion of model 3 when projected at supersonic speeds in the
Langley free-flight apparatus.

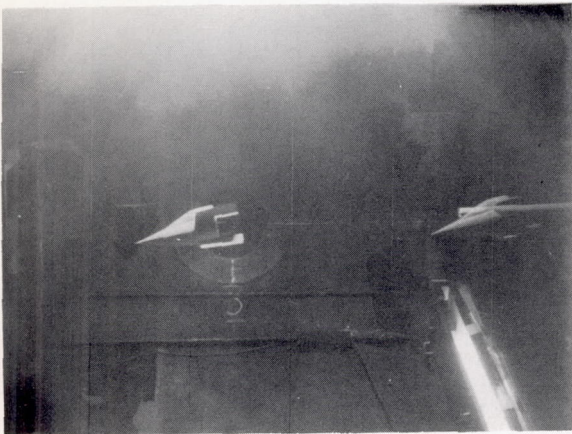Figure 13.- Shadowgraph of model 3 in flight. Mach number, 1.21.
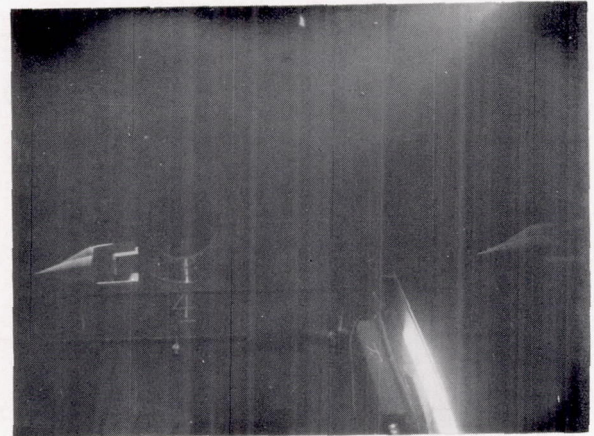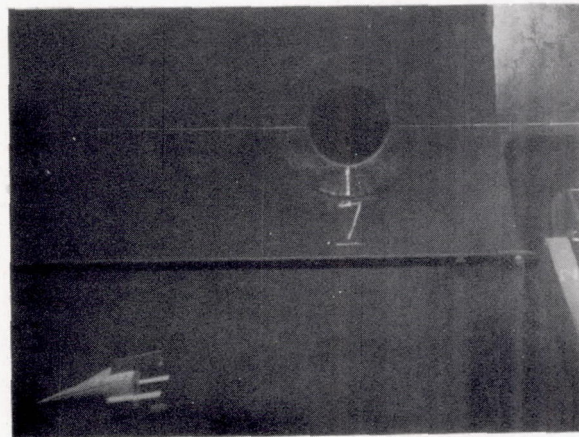
Station 1

Station 2

Station 3

Station 4

Station 7

NACA
L-63045

Direction of travel

Figure 14.- Motion of model 4 when projected at supersonic speeds in the Langley free-flight apparatus. (Cameras at stations 5 and 6 failed.)